Chemical Geology 500 (2018) 175–181

Contents lists available at ScienceDirect

Chemical Geology

journal homepage: www.elsevier.com/locate/chemgeo

Hydrogen and D/H analysis of apatite by Elemental Analyzer-Chromium/High-Temperature Conversion-Isotope Ratio Mass Spectrometry (EA-Cr/HTC-IRMS)

James P. Greenwood

Department of Earth & Environmental Sciences, 265 Church St., Wesleyan University, Middletown, CT 06459, USA

ARTICLE INFO

Editor: Michael E. Böttcher

Keywords:
Apatite
Hydrogen isotopes
SIMS
TC/EA
HTC
Adsorbed moisture

ABSTRACT

Hydrogen and δD measurements of the mineral apatite have been used to measure volatile contents of planets and planetesimals and to infer the sources and evolution of water throughout the solar system. All of these studies use Secondary Ion Mass Spectrometry (SIMS) which necessitates the use of apatite mineral standards to correct for matrix effects, which have previously been measured by mass spectrometry for hydrogen isotopes. Here we present a new technique of Elemental Analyzer-Chromium/High Temperature Conversion-Isotope Ratio Mass Spectrometry (EA-Cr/HTC-IRMS) for the measurement of hydrogen and hydrogen isotopes of apatite. This technique presents greater technical advantages over TC/EA due to ability of chromium to bind with phosphorus in the high-temperature reactor, and prevent this elemental P from clogging the instrument components. We also show that removal of adsorbed moisture of nominally hydrous minerals and glasses becomes increasingly important with decreasing grain size of materials and present experiments on moisture removal from nominally anhydrous quartz. We report hydrogen and hydrogen isotope results of five fluorapatite and two hydroxylapatite samples, including Durango apatite. We show that our results of hydrogen content of Durango apatite are similar to published values using the TC/EA technique. Our recommended values for hydrogen using a Cr reactor for H_2O and $\delta D_{VSMOW\text{-}SLAP}$ for Durango apatite are 608 ± 102 ppm H_2O and $\delta D_{VSMOW\text{-}SLAP} = -86 \pm 4‰$ (2σ).

1. Introduction

Apatite ($Ca_5(PO_4)_3(F,Cl,OH)$) is the only volatile-bearing mineral common in solar-system materials, being found in bodies both large (Earth, Moon, Mars) and small (chondrites and achondrites) (McCubbin and Jones, 2015a). It is the main igneous phosphate mineral on the Earth (Piccoli and Candela, 2002), and along with the anhydrous Ca-phosphate mineral merrillite, is the main igneous phosphate mineral in the Moon (Fuchs, 1970) and Mars (Fuchs, 1969). The use of apatite to investigate volatile abundances of other planets was pioneered by Watson et al. (1994) in their study of water and D/H of martian meteorites. The measurement of hydrogen in apatite was used to determine the first high water abundances of lunar materials (Boyce et al., 2010; McCubbin et al., 2010a, 2010b) and the D/H of apatite to determine the unique extraterrestrial signature of the Moon (Greenwood et al., 2011). These pioneering studies of the hydrogen and D/H in the Moon and Mars have led to a number of SIMS studies using apatite to understand water and hydrogen isotope distributions of the Moon (Barnes et al., 2013; Tartése and Anand, 2013; Tartèse et al., 2013, 2014a, 2014b; Boyce et al., 2014; Robinson and Taylor, 2014; Robinson et al., 2016; Singer et al., 2017), Mars (Leshin, 2000; Boctor et al., 2003; Greenwood et al., 2008; McCubbin et al., 2012; Hallis et al., 2012), Vesta (Sarafian et al., 2014, 2016), the angrite parent body (Sarafian et al., 2017), ordinary chondrites (Jones et al., 2014, 2016) and R chondrites (McCanta et al., 2008).

Apatite was not used to investigate water and hydrogen isotopes in terrestrial magmas until Nadeau et al. (1999), and they only studied apatites from alkaline intrusive complexes, not a global study. The first SIMS studies of hydrogen in apatite showed that volatile distributions of apatite could be used to track late-stage magmas in volcanoes (Boyce and Hervig, 2008, 2009). Other studies have used apatite to track late-stage history of S, F, and Cl in volcanoes (Dietterich and de Silva, 2010; Scott et al., 2015), but the potential of using hydrogen and hydrogen isotopes of apatite for terrestrial problems remains largely untapped.

The studies of water and hydrogen isotopes of apatite in extraterrestrial samples have all used Secondary Ion Mass Spectrometry (SIMS) due to the small masses of these precious materials in our museums and collections. SIMS analysis of hydrogen and deuterium (or other volatile masses) requires the use of apatite standard minerals, determined by mass spectrometry for H and D/H, or FTIR for hydroxyl,

E-mail address: jgreenwood@wesleyan.edu.

https://doi.org/10.1016/j.chemgeo.2018.09.029
Received 19 January 2018; Received in revised form 27 August 2018; Accepted 22 September 2018
Available online 01 October 2018
0009-2541/

and electron microprobe for fluorine and chlorine and other chemical elements. Studies of hydrogen in Martian apatite, combined with experimental petrology, are used to determine the mantle water content of Mars (McCubbin et al., 2012), and highlight the importance of properly determined amounts of hydrogen in apatite standard minerals for SIMS analyses. Watson et al. (1994) used apatite measured in the lab of Samuel Epstein using vacuum pyrolysis and a Nier-type double collector gas source mass spectrometer. Nadeau et al. (1999) made the first published measurements of hydrogen and D/H in apatite, and describe a stepped-heating method to release water from apatite and inlet it to the same mass spectrometer in the lab of Samuel Epstein. They found that temperatures > 800 °C were needed to release hydroxyl from apatite with grain sizes > 45 μm. They also found that some apatite minerals required extended time at 1500 °C (> 24 h) to release structural OH in their system (Nadeau et al., 1999). This is likely due to slow diffusivity of hydrogen in apatite (Higashi et al., 2017). The advent of methods for measuring water in minerals using Continuous Flow Isotope Ratio Mass Spectrometry (CF-IRMS) (Sharp et al., 2001), led Greenwood et al. (2008) to use the Thermo Finnigan TC/EA HTC (High Temperature Conversion) coupled to CF-IRMS to measure hydrogen and D/H of apatite. This method was also used to determine hydrogen and δD for apatite minerals by Greenwood et al. (2011) and McCubbin et al. (2012).

Here we present a new method for determining the hydrogen mass fraction and δD of fluorapatite and hydroxylapatite using a Cr-based reactor coupled to a Thermo Scientific Delta Advantage that offers significant technical advantages over the TC/EA HTC glassy carbon method. A major advantage of this technique is the ability of Cr metal to bond with P and serve as a getter for this analytical byproduct (Gehre et al., 2015), as the efficiency of measuring phosphates by CF-IRMS is severely hampered if this byproduct makes it downstream to other components of the system. Variations of this method have been previously applied to organic compounds (Gehre et al., 2015; Renpenning et al., 2015; Nair et al., 2015), halogen- and sulfur-bearing organic compounds (Gehre et al., 2017) and hydrous minerals and waters (Qi et al., 2017).

2. Experimental Methods

Hydrogen mass fraction and δD measurements were made using the Wesleyan Hydrogen Isotope Mass Spectrometer (WHIMS), which consists of a HTC (TC/EA, Thermo-Finnigan, Bremen, Germany) reduction unit equipped with a Costech Zero-blank 50-position autosampler (Costech, Valencia, California), a Finnigan ConFlo III gas introduction system (Thermo Electron, Bremen, Germany), and a Delta V Advantage isotope ratio mass spectrometer (Thermo Fisher Scientific, Bremen, Germany). We have modified the autosampler by adding a vacuum system to assist in removing adsorbed moisture of samples before analysis (G. St. Jeans, pers. comm.).

The glassy carbon-filled reactor of the TC/EA was modified by adding a layer of 2 mm grain size Cr-metal chips as first advocated by Gehre et al. (2015). We have modified their published reactor (which was designed for organics) by keeping the glassy carbon reduction tube, and have this tube in an alumina tube. A diagram of the reactor packing is shown in Fig. 1. From bottom to top, a 470 mm length alumina tube is packed with 1 mm of silver wool, 20 mm of quartz wool, and 36 mm of glassy carbon chips. The 360 mm length glassy carbon tube rests on this, and is packed from bottom to top by 5 mm of silver wool, 88 mm of glassy carbon chips, 15 mm layer of 2 mm grain size Cr metal chips, and 5 mm of glassy carbon chips. In the hot zone is a #4 round graphite crucible 30 mm in height. The top of the crucible is 270 mm from the top of the alumina tube. We experimented without a crucible, but unfortunately we are often making basalt as a byproduct of other work on hydrogen in silicate glasses, which leads to the rapid destruction of expensive glassy carbon tubes.

The He carrier gas was fed from the top (110 ml/min), as originally

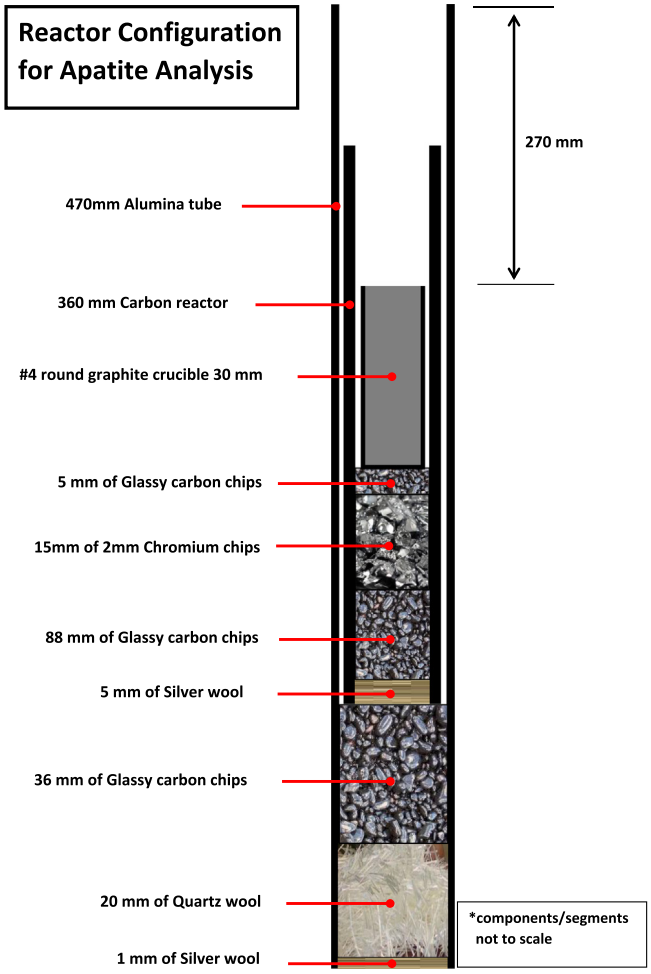

Fig. 1. Schematic of Cr-EA reactor assembly for apatite analyses. Not drawn to scale.

supplied. We ran the HTC reactor at 1450 °C with the gas chromatograph at 90 °C. The gas chromatograph was 6 m × 0.635 cm × 4 mm stainless steel packed with 80–100 mesh 5A molecular sieve. The He flow rate at the GC output was 209 μl/min. We also used a sequence of traps to try to contain the elemental phosphorus contaminant. After the reactor, we installed a CO_2-H_2O trap containing Mg-perchlorate and CO_2 adsorbent. A second trap is located after the GC, which is a coiled stainless steel tube in LN_2.

Due to the lack of suitable apatite hydrogen isotope reference materials, and until recently the lack of hydrous mineral hydrogen isotope reference materials (Qi et al., 2017), we used reference waters encapsulated in silver tubes (Qi et al., 2010) to correct apatite hydrogen isotope data. Reported values of δD in this study are corrected using VSMOW, GISP, and SLAP, and are also $\delta^2H_{VSMOW\text{-}SLAP}$ values. The waters are analyzed before or after unknown apatite minerals due to the stringent drying requirements required for analyzing nominally hydrous minerals such as fluorapatite (see below).

Measurements of hydrogen mass fraction in apatite were corrected by using our internal kaolinite ($Al_2Si_2O_5OH_4$) mineral standard (WES-1). This kaolinite was purchased from Wards Scientific and processed in our lab for use as an in house standard for hydrogen. Bulk sample was ground in an agate mortar and pestle, and then sieved to collect the 20–32 μm fraction. We found this removed most mineral contaminants in the sample using binocular microscopy. The kaolinite is kept in a desiccator until needed. The 20–32 μm fraction is weighed out to sample sizes typically ranging from 50 to 450 μm in 50 μm increments to ± 1 μg with a Mettler Toledo MX5 microbalance, and then

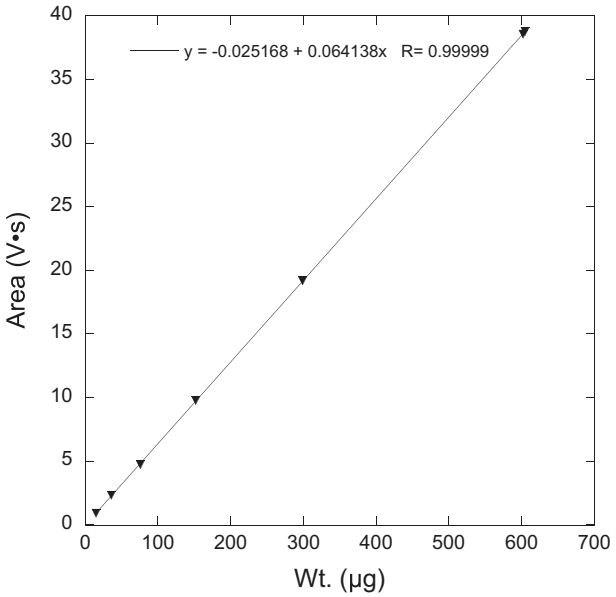

Fig. 2. Area (V·s) vs. wt. (µg) of internal standard WES-1 kaolinite. Linear fit and equation shown. This is a typical regression analysis of different weights of kaolinite that would be used to determine hydrogen mass fraction of apatite during analytical runs.

encapsulated in 3.5 × 5 mm silver cups. These are then loaded into the autosampler, pumped under rough vacuum for 30 min, and then followed by 15 min He purge. Regression analysis of the six to eight kaolinite samples is used for our hydrogen mass standard. An example of a kaolinite regression is shown in Fig. 2. The hydrogen mass fraction of stoichiometric kaolinite is 1.561 wt% hydrogen. We confirmed that our kaolinite has 1.561 wt% hydrogen using USGS62 caffeine as done by Qi et al. (2017) (See Supplementary Materials Table S1).

3. Sample preparation

We chose five fluorapatites for this study (Buckingham, Quebec, Canada; Durango, Cerro Mercado, Mexico; Lake Baikal, Sludyanka, Russia; Morocco (from S. Itoh); Zillertal, Austria) and two hydroxylapatites from Minas Gerais, Brazil (Linopolis and Sapo Mine). For this work, large single crystals of apatite were used, except for Linopolis, Brazil, which consisted of mm-sized crystals picked from one large hand specimen. All apatite minerals were chosen for their gem-like clarity which indicates a lack of fluid inclusions. The Linopolis sample is the least water-clear of the samples, and is a translucent to milky blue-green. After closer inspection with binocular microscopy for contaminants, apatite minerals are reduced to the 20–32 µm sieve fraction through a process of gentle crushing and grinding with an agate mortar and pestle to minimize production of the < 20 µm fraction. After further binocular microscope inspection, the samples are transferred to a Gilson 3″ stainless steel (SS) sieve tower and shaken with a Gilson Performer III vibrating shaker for 30 min. Upon completion of the sieving process, the 20–32 µm fraction is rinsed with 18 MΩ deionized water multiple times until water-clear, to remove the statically bound < 20 µm particles. The washed sample is then dried under vacuum.

After drying, the 20–32 µm apatite sieve fraction is weighed in a microbalance. Due to the low water contents of apatite, up to 40 mg of sample were weighed into 4 × 6 mm silver capsules, and then pressed with custom SS convex/concave hand tools into a sphere to remove trapped air. These small silver spheres are then pierced with a 27G syringe needle to enable adsorbed moisture release, and then placed in an aluminum 96 well sample tray. These trays are then placed in a Thermolyne Muffle furnace at 400 °C for 1 h with no vacuum. Afterwards, samples are removed and quickly transferred to the sample carousel of the Zero-blank autosampler. At this point, in-house kaolinite samples are loaded just prior to apatite to run a regression for hydrogen and the kaolinite is also loaded as an unknown interspersed among the apatite samples to check for drift during the mass spectrometric analyses. Apatite and kaolinite are then pumped with a roughing vacuum for 15 min in the autosampler, followed by a 15 min He purge.

The choice of drying temperature and time were guided by the fact that 400 °C is too low a temperature to remove significant structural OH from apatite, due to low diffusivity of hydrogen in this mineral (Higashi et al., 2017). We found that rough vacuum pumping alone was insufficient to dry 40 mg of 20–32 µm apatite grains, even combined with low temperature heating (< 200 °C). In a study of hydrogen in mantle garnets by TC/EA, a drying time of 350 °C for 4 h was found necessary to remove adsorbed water (Gong et al., 2007). We undertook a study of drying of quartz with different grain sizes to find adequate conditions for drying apatite (See Results).

4. Results

4.1. Adsorbed moisture removal

Martin et al. (2017) reported that water and hydrogen isotopic values are compromised for the finest size fractions of volcanic glasses due to adsorbed water. To study the removal of adsorbed moisture, a single crystal of water-clear quartz was ground and sieved under the same conditions described for apatite above. Results of tests of adsorbed water on anhydrous quartz with different size sieve fractions and sample masses are shown in Fig. 3. All samples that were not baked for 1 h at 400 °C (not under vacuum), but were instead submitted to a ~15 min He purge in the Zero-blank autosampler (normal conditions for TC/EA analysis of solids), had high, measurable water contents. The grain size effect can be seen clearly in the unbaked samples of 10 mg mass, where water content increases with surface area: The 32–45 µm

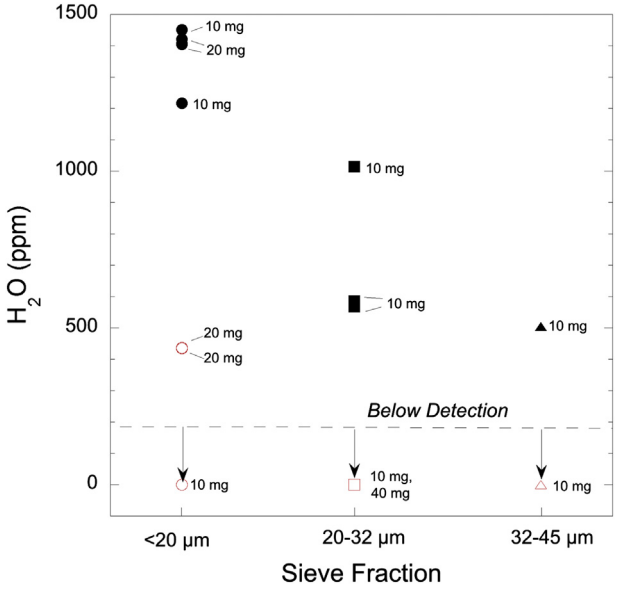

Fig. 3. H_2O (ppm) vs. sieve fraction of anhydrous quartz. Closed, black symbols represent samples that were not baked or vacuum-dried, but only purged with He for 15 min. Open, red symbols represent samples that were baked for 1 h at 400 °C (not under vacuum) to remove adsorbed moisture. Sample masses are listed next to the analyses. For the conditions of low water fluorapatite analyses, 40 mg of sample at 20–32 µm sieve fraction, a bake at 1 h at 400 °C is sufficient for removal of adsorbed water. Circles: < 20 µm sieve fraction; Squares: 20–32 µm sieve fraction; Triangles: 32–45 µm sieve fraction. (For interpretation of the references to colour in this figure legend, the reader is referred to the web version of this article.)

fraction has ~500 ppm H_2O, the 20–32 μm fraction ~1000 ppm H_2O, and the < 20 μm fraction approaching 1500 ppm H_2O.

When the quartz sieve fractions are baked for 1 h at 400 °C (not under vacuum), the water contents are seen to dramatically decrease. For 10 mg sample masses, no water peak is observed for the three size fractions studied. For 20 mg samples of the < 20 μm size fraction, a water content approaching 500 ppm is observed. For the conditions of low water content apatites, such as Durango, Buckingham, and Lake Baikal, 40 mg of 20–32 μm size fraction quartz did not generate a detectable peak, but a small bump can be seen up to 2× background for a small time window. This adsorbed water signal is not considered, since we cannot quantify it. The kaolinite regression shown in Fig. 2 shows that very low water contents can potentially be measured with this method (the lowest kaolinite mass is 15 μg in Fig. 2, suggesting a detection limit < 10 ppm H_2O).

4.2. Reaction of apatite in HTC at 1450 °C

Nadeau et al. (1999) showed that some apatite samples required temperatures in excess of 1500 °C for 24 h to remove structural hydroxyl. To investigate the behavior of apatite in the HTC reaction, we undertook an experiment to mimic the beginning of a typical apatite run sequence. Five kaolinites, three Sapo Mine hydroxylapatites, one Durango 60 fluorapatite, and two quartz samples loaded into the Zeroblank autosampler, pumped under rough vacuum for 30 min, and then purged with He for 15 min. The samples were then run under normal conditions, and then cooled and the crucible removed. The contents of the crucible were carefully removed and mounted for Scanning Electron Microscope (SEM) observations. All apatite samples in this experiment show evidence of melting and formation of new phases during the HTC reaction. Cr-bearing Barringerite $(Fe,Ni)_2P$ is tentatively identified in all apatite samples of this experiment, demonstrating that apatite PO_4 is being reduced. Cl-bearing britholite $(Ca_5(P,Si)O_4)_3OH,F$ and Cl-free apatite are also found in the experiment. An example of the reaction product from the second Sapo Mine sample in the experiment is shown in Fig. 4.

Our mass spectrometer observations of hydrogen extraction from apatite also appear to confirm that hydroxyl is removed effectively during the HTC reaction time of 3 min. We do not observe an increase in background for mass 2 during any of the runs reported in this manuscript. If apatite was slowly decomposing and losing hydroxyl over time, the background should have been increasing at some point during the large runs of apatite samples, but this was not seen.

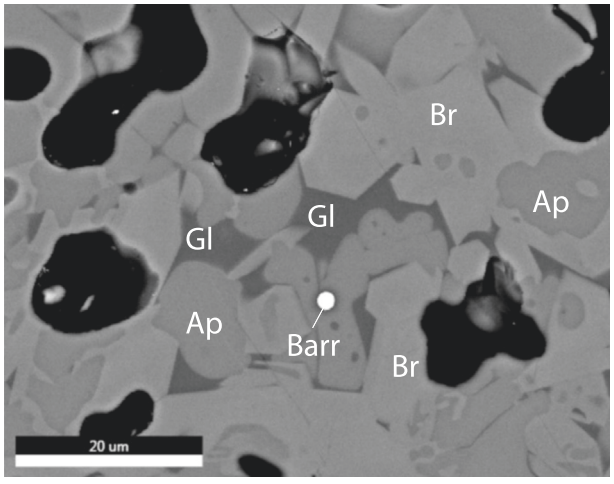

Fig. 4. Backscatter electron image of experimental run products from Sapo Mine. Fluorapatite (Ap) is Cl-free. Cl-, F-bearing britholite-like phase (Br) is the majority of the sample (Si:P of 35:65). Cr-bearing iron-nickel phosphide barringerite is also present demonstrating reduction of original apatite. Glass is calcium-alumino-silicate rich.

4.3. Mass fraction of hydrogen in fluorapatite

The mass fraction of hydrogen (H%) of three single crystals of Durango apatite are shown in Table 1. The three crystals of Durango (designated Dur60, Dur63, and DurRR) were run in several analytical sessions. Due to the difficulty in releasing hydrogen from apatite (Nadeau et al., 1999), peaks were broad for Durango apatite. Though the amplitudes on mass 2 are low (< 750 mV), water content is reproducible within individual runs (Table 1). These areas of Durango apatite are also within the range of areas analyzed for the kaolinite regression in these same runs (e.g. Fig. 2). All samples are run in triplicate, and the first sample is disregarded due to possible memory effects. We did not actually observe any memory effects for hydrogen mass fraction or hydrogen isotopes, but followed this procedure always. Shown in Table 1 are the two replicate analyses, and their corrected mean hydrogen as H_2O (ppm) with error as two standard deviations (2σ). While the three apatite crystals suggested possible different water contents (DurangoRR had the most H_2O and Durango60 the least H_2O in each run), we cannot resolve the possible water differences between these crystals with our current analytical technique. We instead pool the analyses for all three crystals and report the mean H_2O for Durango apatite of 608 ± 102 ppm (2σ) (n = 14).

The hydrogen mass fraction, as %H and H_2O ppm, for fluorapatite samples Buckingham, Russia(#2), and Zillertal are listed in Table 2. The Buckingham apatite has 905 ± 6 ppm H_2O (2σ) (n = 4) and Zillertal apatite has 5274 ± 394 ppm H_2O (2σ) (n = 2). Our single crystal of Russia apatite from Lake Baikal (Russia#2) has 1604 ± 14 ppm H_2O (2σ) (n = 2). We note that earlier measurements on another apatite crystal (Russia#1) had almost 2× the hydrogen content of Russia#2 (not shown), thus suggesting some heterogeneity in apatite from this locality.

4.4. Mass fraction of hydrogen and $\delta D_{VSMOW\text{-}SLAP}$ of fluorapatite and hydroxylapatite

In Table 3, we report the mass fraction of hydrogen and $\delta D_{VSMOW\text{-}SLAP}$ of fluorapatite crystals for runs with mass 2 > 1000 mV. Also reported are the results of Russia#2 using a different Cr reactor assemblage (Cr50/50) after Gehre et al. (2017), designed to deal with halogen byproducts. In Table 4, we report the mass fraction of hydrogen and $\delta D_{VSMOW\text{-}SLAP}$ of two hydroxylapatite samples from Minas Gerais, Brazil, denoted Linopolis and Sapo Mine. These two high water content samples always had sufficient signal for hydrogen isotope analyses. The two samples are quite heterogeneous in water content with Linopolis having 1.26 ± 0.24 H_2O wt% (2σ) (n = 4) and Sapo Mine at 1.43 ± 0.14 wt% H_2O (2σ) (n = 4).

5. Discussion

5.1. Comparison of HTC reactors: Cr vs. Glassy Carbon vs. Cr 50%/Glassy Carbon 50%

The addition of the Cr metal to the glassy carbon reactor was done primarily to reduce the downstream contamination of the system by elemental phosphorus, a reaction product of phosphates in the TC/EA. Due to the high masses of apatite required to achieve sufficient signal, prior to the use of Cr metal, we would need to change out all components between the reactor and the mass spectrometer (capillaries, traps, GC, open splits, stainless steel tubing) after only ~100 analyses due to elemental phosphorus contamination. Before introduction of the Cr method, after phosphate analyses for hydrogen on the glassy carbon reactor of the TC/EA, the stainless steel trap would be heated and a valve used to send the trapped material to vent. After a few minutes, a small white flame at the exit of the stainless steel tube would appear

Table 1
Hydrogen mass fraction of three large single crystals of fluorapatite from Durango, Mexico. Error is 2σ (n = 2), unless otherwise noted. Hydrogen amount is corrected to our internal Kaolinite standard (WES-1). Reactor is Cr and is shown in Fig. 1.

Run	Durango60			DurangoRR			Durango63		
	%H	Area (V·s)	H_2O (ppm)	%H	Area (V·s)	H_2O (ppm)	%H	Area (V·s)	H_2O (ppm)
1	0.00627	8.87	561*	0.00689	9.77	615 ± 22	–	–	–
2	0.00616	8.46	551 ± 2	0.00680	9.36	608 ± 26	–	–	–
3	–	–	–	–	–	–	0.00682	10.06	609 ± 30
4	0.00694	7.84	621 ± 2	0.00790	9.12	706 ± 100	0.00768	8.82	686 ± 16
7	0.00635	5.55	567 ± 38	0.00726	6.57	648 ± 8	0.00683	6.16	610 ± 18
9	0.00596	5.83	532 ± 2	0.00722	7.07	645 ± 12	0.00623	6.10	557 ± 12
	Mean H_2O = 566 ± 64 (n = 5)			Mean H_2O = 644 ± 78 (n = 5)			Mean H_2O = 615 ± 106 (n = 4)		
Mean H_2O of above analyses of 3 Durango Crystals: 608 ± 102 ppm (n = 14)									

* n = 1.

and persist for at least 15 min while heating the trap with a heat gun. This is common after analyzing silver phosphate via TC/EA for oxygen isotopes as well (G. Olack, pers. comm.). After implementing the Cr method, this phenomenon disappeared.

The 50% Cr and 50% glassy carbon reactor (Gehre et al., 2017) was also assessed, due to the concern that halogens from apatite reaction could be causing HX (X = halogen) reaction byproducts in the 2 cm Cr layer used in the reactor assemblage of this study (Fig. 1). Russia#2 apatite was run using a 50% glassy carbon/50% Cr reactor (as described in Gehre et al., 2017), and results in Table 3 for hydrogen as H_2O are similar to runs using the Cr reactor assemblage described in this paper. The runs from both reactors in Table 3 are similar to runs of Russia#2 in Table 2. This suggests that either reaction assemblage is appropriate for analyzing hydrogen mass fraction of apatite minerals. The reaction byproducts of Cl-bearing fluorbritholite and Cl-free fluorapatite in the melting experiments described in Section 4.2 also suggest that downstream formation of HX compounds may be inhibited by reaction byproducts of halogens in hotzone of the HTC in our runs of apatite minerals.

5.2. Release of hydrogen from apatite in HTC reactor at 1450 °C

Our run sequences for the analysis of hydrogen in apatite minerals always begins with a sequence of six to eight kaolinite samples of different weights to establish the regression analysis for amount % hydrogen. The first apatite samples react with the dehydrated kaolin in the crucible to make an alumino-silicate-phosphate melt, that is reducing enough to also have the phosphide mineral barringerite (Fig. 4). The reaction byproducts suggest complete breakdown of original apatite minerals during the HTC reaction at 1450 °C. The mass spectrometric observations of no changes in backgrounds for masses 2 and 3 after an individual apatite analysis, and throughout a run sequence of apatite samples, are also consistent with nearly complete release of hydroxyl from apatite during the ~3 min HTC reaction.

5.3. Comparison of results with previous work

We can compare our results to the published literature on apatite water and δD values. We first compare our results on Durango and Linopolis apatite to our own published results (Greenwood et al., 2008, 2011). Greenwood et al. (2008) reported 480 ppm H_2O for Durango apatite and for Linopolis apatite 1.24 wt% H_2O and δD = −116 ± 4‰ (1σ). This result compares very favorably with the water content of Durango apatite in Table 1 (608 ± 102 ppm H_2O for three Durango crystals) and the water content of Linopolis in Table 4 (1.26 ± 0.24 wt % H_2O). The δD of Linopolis is also within error of the values in Table 4 (δD: −111 ± 6‰). Greenwood et al. (2008, 2011) used the TC/EA technique with glassy carbon. Apatite grains were ground to a fine powder to accentuate release of hydrogen during HTC pyrolysis at 1450 °C.

Greenwood et al. (2011) published updated values for Durango and Linopolis based on continued TC/EA work on apatite hydrogen. The water content of Durango remained essentially unchanged at 478 ppm H_2O, but with a δD = −120 ± 5‰. This hydrogen isotope value appears unsupported by the data presented in Table 3 (two Durango apatite crystals: −87 ± 1‰ and −85 ± 6‰). Due to inadequate TC/EA drying techniques, it is likely adsorbed water that is causing the light hydrogen isotope value for Durango apatite in Greenwood et al. (2011), and this δD value of −120 ± 5‰ should not be used. The values for Linopolis apatite in Greenwood et al. (2011) are 1.57 wt% H_2O and δD = −125 ± 5‰. This high water content for Linopolis apatite is just outside the range reported in Table 4 for this apatite sample (1.26 ± 0.24 wt%; 2σ). The higher water content could be a result of sample heterogeneity (see Table 3) or poor control on hydrogen content due to hydrogen mass fraction being determined from benzoic acid in these early studies of Greenwood et al. (2008) and (2011). The hydrogen isotope value of Linopolis of −125 ± 5‰ is outside the range of −111 ± 5‰ (2σ) reported here (Table 4). The recommended hydrogen isotope value for Linopolis is: δD = −111 ± 6‰ (2σ) (Table 4).

McCubbin et al. (2012) published glassy carbon TC/EA analyses of

Table 2
Hydrogen mass fraction of fluorapatite from Buckingham, Quebec, Zillertal, Austria, and Lake Baikal, Russia. Error is 2σ (n = 2), unless otherwise noted. Hydrogen amount is corrected to our internal Kaolinite standard.

Run	Buckingham, Quebec, CA			Zillertal, Austria			Russia (#2), Lake Baikal		
	%H	Area (V·s)	H_2O (ppm)	%H	Area (V·s)	H_2O (ppm)	%H	Area (V·s)	H_2O (ppm)
3	0.01015	15.09	907 ± 6	–	–	–	–	–	–
5	0.01015	14.65	907 ± 18	–	–	–	–	–	–
6	0.01013	13.70	905 ± 24	–	–	–	0.01800	15.22	1609 ± 8
8	0.01007	10.12	900 ± 11	–	–	–	0.01789	11.28	1599 ± 15
9	–	–	–	0.06249	15.29	5585 ± 14	–	–	–
10	–	–	–	0.06561	25.13	5863 ± 18	–	–	–
	Mean H_2O = 905 ± 6 (n = 4)			Mean H_2O = 5724 ± 394 (n = 2)			Mean H_2O = 1604 ± 14 (n = 2)		

Table 3
Hydrogen mass fraction (as H_2O ppm) and $\delta D_{VSMOW\text{-}SLAP}$ of fluorapatite crystals. Error is 2σ (n = 2) unless otherwise noted. The average amplitude of mass 2 (Amp.) is reported in mV.

Sample	Location	Reactor	Run	Amp. (mV)	H_2O (ppm)	$\delta D_{VSMOW\text{-}SLAP}$ (‰)
Buckingham	Quebec	Cr	11	1933	913 ± 108	−87 ± 2
Durango60	Mexico	Cr	11	1785	650 ± 24	−85 ± 6
DurangoRR	Mexico	Cr	11	1679	737 ± 18	−87 ± 1
Russia(#2)	Lake Baikal	Cr	11	1491	1517 ± 70	−67 ± 3
Russia(#2)	Lake Baikal	Cr50/50	12	1061	1498 ± 22	−73 ± 1
Russia(#2)	Lake Baikal	Cr50/50	13	978	1555 ± 10	−75 ± 2
Zillertal	Austria	Cr	5	1057	5560 ± 258	−72 ± 1
Zillertal	Austria	Cr	6	1094	5664 ± 28	−71 ± 1
				Mean	5612 ± 148	−72 ± 2 (n = 2)
Shoichi	Morocco	Cr	5	2643	3840 ± 288	−77 ± 4
Shoichi	Morocco	Cr	6	2853	3963 ± 264	−79 ± 1
Shoichi	Morocco	Cr	8	1892	3596*	−85*
Shoichi	Morocco	Cr	11	4700	3645 ± 298	−64 ± 2
				Mean	3761 ± 342	−76 ± 17 (n = 4)

* n = 1.

Table 4
Hydrogen mass fraction (as H_2O wt%) and $\delta D_{VSMOW\text{-}SLAP}$ of hydroxylapatite crystals. Error is 2σ (n = 2) unless otherwise noted. Internal error for H_2O is generally less than reported significant figures. Reactor is Cr as shown in Fig. 1.

Sample	Location	Run	H_2O (wt%)	$\delta D_{VSMOW\text{-}SLAP}$ (‰)
Linopolis	Brazil	4	1.09	−115 ± 1
Linopolis	Brazil	7	1.27	−109 ± 1
Linopolis	Brazil	8	1.37	−111 ± 1
Linopolis	Brazil	11	1.32	−109 ± 3
			Mean: 1.26 ± 0.24	−111 ± 6 (n = 4)
Sapo Mine	Brazil	5	1.45 ± 0.03	−112 ± 1
Sapo Mine	Brazil	7	1.33	−114 ± 3
Sapo Mine	Brazil	8	1.47	−112 ± 4
Sapo Mine	Brazil	11	1.48 ± 0.03	−109 ± 1
			Mean: 1.43 ± 0.14	−112 ± 4 (n = 4)

hydrogen in apatite, and two of their apatite samples may be similar to samples analyzed here. Their Ap003 is from Durango, Mexico, and Ap018 is from Lake Baikal, Russia. They report 600 ± 400 ppm for Durango and 2000 ± 400 ppm for Lake Baikal, Russia. This is very similar to the values we report in Table 1 for Durango apatite (608 ± 102 ppm H_2O for three Durango crystals). We also see similar results for the Lake Baikal apatite (Tables 2 and 3), but we note that we did see heterogeneity in water content between our apatite samples from this locale. McCubbin et al. (2012) report a δD = −90 ± 3‰ for their sample of Lake Baikal apatite, which is very different than our measurement of Lake Baikal apatite (δD = −72 ± 8‰; Table 3), suggesting that these two samples are not related to each other, and there is heterogeneity in samples from this locale in hydrogen isotopes as well.

Two higher water content values for Durango apatite were published by McCubbin et al. (2010a) and Boyce et al. (2010) of 900 ± 200 and 1170 ± 117 ppm H_2O, respectively. The 900 ± 200 ppm value is a manometric value (McCubbin et al., 2010a), and Boyce et al. (2010) determined via SIMS calibration pinned to a measurement of Mud Tank apatite from Nadeau et al. (1999). These values appear too high compared to the values for three Durango crystals in Table 1, as well as Greenwood et al. (2008, 2011), and McCubbin et al. (2012), but sample heterogeneity cannot be ruled out.

5.4. Implications for SIMS studies of hydrogen in apatite

In our SIMS work on apatite standards (Greenwood et al., 2008, 2011) we have determined the water content of extraterrestrial apatites by using the $^1H/^{18}O$ ratio of extraterrestrial apatite vs. that of Durango and Linopolis apatites. Typically, for extraterrestrial work on volatile contents of other solar system materials, the hydrogen mass fraction of the standard minerals is more important than δD. This is because the internal error for δD SIMS measurements can be as large as the entire range of the natural δD of terrestrial minerals (e.g. Greenwood et al., 2011; Barnes et al., 2013). Using the apatite minerals studied here, SIMS calibration curves for hydrogen using Buckingham and Zillertal apatite in the same mount were achieving calibration curves with a zero y-intercept (S. Itoh, pers. comm.), which is a significant improvement over presently available apatite SIMS standard minerals. I have a large supply of apatite from Buckingham, Quebec, CA, but only limited supply of apatite from Zillertal, Austria. I hope to obtain more of the Zillertal apatite, and will analyze it with the procedures outlined in this study, and will hopefully be able to make this available to other SIMS researchers in the near future.

6. Conclusions

I have developed a new EA-Cr/HTC-IRMS method for the determination of hydrogen and δD in apatite-group minerals. This method uses Cr as a getter for P in the HTC reactor which increases instrument uptime by containing the elemental phosphorus to the reactor instead of contaminating downstream components such as the GC and causing capillaries to stick in the open split of the ConFlo III. Analyses of hydrogen mass fraction in two apatites (Durango and Lake Baikal) are within error of literature values obtained with the glassy carbon reactor in the TC/EA method (Greenwood et al., 2008; McCubbin et al., 2012).

For the analysis of nominally hydrous minerals and glasses (~ < 3000–5000 ppm H_2O), proper removal of adsorbed moisture is critical to obtaining accurate hydrogen mass fractions. I found that even for the drying conditions of 1 h at 400 °C, the < 20 μm sieve fraction of nominally anhydrous quartz had a mass fraction of hydrogen of 500 ppm as H_2O. 40 mg of 20–32 μm sieve fraction of quartz did not generate a detectable peak for hydrogen and was the sample mass and sieve fraction of apatite used for all measurements reported in this study.

The EA-Cr/HTC and TC/EA methods that use a temperature of reaction of 1450 °C are recommended for apatite, as well as the use of a glassy carbon tube to aid in sample reduction. We use a regression sequence of kaolinite that we run directly before apatite minerals in our run sequences, and we find apatite melts in the crucible under these conditions in the system described herein. The melting of apatite likely enhances the release of hydrogen in the short time of the HTC reaction (~3 min) and allows for quantitative hydrogen release.

We report the hydrogen mass fraction of five fluorapatite and two hydroxylapatite minerals from different localities, including three that have values in the published literature. We find good agreement with literature values and the values presented in this study for these three

samples. The use of Durango apatite as a SIMS standard for hydrogen analyses is prevalent in the community. This study finds that three crystals of Durango apatite have hydrogen mass fraction (as H_2O) of 608 ± 102 ppm (n = 14). Our recommended hydrogen isotope value for Durango apatite is: $\delta D_{VSMOW\text{-}SLAP} = -86 \pm 4‰$ (2σ).

Supplementary data to this article can be found online at https://doi.org/10.1016/j.chemgeo.2018.09.029.

Acknowledgements

I thank Jim Zareski for his tireless efforts since 2014 in maintaining the WHIMS instrument and developing new and improved techniques to make this study possible. I also thank Gerard Olack for helping with setting up the mass spectrometer facility at Wesleyan and for answering every troubleshooting question we had in 2014–2015, as well as helping getting this work started at Yale a decade ago. I thank Gilles St. Jean for sharing his knowledge of Thermo instrumentation and mass spectrometry. I thank my collaborators on SIMS projects both lunar and martian, Yoshi Yurimoto, Shoichi Itoh, and Naoya Sakamoto, for being patient with the long duration of this study. I thank my collaborators Francis McCubbin, Jeremy Boyce, and Allan Treiman for discussions on apatite. Kenichi Abe is thanked for assisting with SEM analysis. Reviews of the manuscript by I. Bindemann and an anonymous reviewer contributed immensely to the quality of this manuscript. I thank Wesleyan University for providing the funds to purchase the WHIMS instrument. NASA-LASER grants (NNH09ZDA001N and NNX14AQ76G) to JPG are acknowledged for funding this apatite standard calibration effort. NSF-MRI (1724591) provided funding for the Wesleyan University FE-SEM instrument used in this effort.

References

Barnes, J.J., Franchi, I.A., Anand, M., Tartèse, R., Starkey, N.A., Koike, M., Sano, Y., Russell, S.S., 2013. Accurate and precise measurements of the D/H ratio and hydroxyl content in lunar apatites using NanoSIMS. Chem. Geol. 337, 48–55.

Boctor, N.Z., Alexander, C.M.O'.D., Wang, J., Hauri, E., 2003. The sources of water in Martian meteorites: clues from hydrogen isotopes. Geochim. Cosmochim. Acta 67, 3971–3989.

Boyce, J.W., Hervig, R.L., 2008. Magmatic degassing histories from apatite volatile stratigraphy. Geology 36, 63.

Boyce, J.W., Hervig, R.L., 2009. Apatite as a monitor of late-stage magmatic processes at Volcán Irazú, Costa Rica. Contrib. Mineral. Petrol. 157, 135.

Boyce, J.W., Liu, Y., Rossman, G.R., Guan, Y., Eiler, J.M., Stolper, E.M., Taylor, L.A., 2010. Lunar apatite with terrestrial volatile abundances. Nature 466, 466–470.

Boyce, J.W., Tomlinson, S.M., McCubbin, F.M., Greenwood, J.P., Treiman, A.H., 2014. The lunar apatite paradox. Science 344, 400–402.

Dietterich, H., de Silva, S., 2010. Sulfur yield of the 1600 eruption of Huaynaputina, Peru: contribution from magmatic, fluid-phase, and hydrothermal sulfur. J. Volcanol. Geotherm. Res. 197, 303–312.

Fuchs, L.H., 1969. The phosphate mineralogy of meteorites. In: Millman (Ed.), Meteorite Research. Springer-Verlag, NY.

Fuchs, L.H., 1970. Fluorapatite and other accessory minerals in Apollo 11 rocks. In: Proc. Apollo 11 Lunar Sci. Conf. pp. 475–479.

Gehre, M., et al., 2015. On-line hydrogen-isotope measurements of organic samples using elemental chromium: an extension for high temperature elemental-analyzer techniques. Anal. Chem. 87, 5198–5205.

Gehre, M., et al., 2017. Optimization of on-line hydrogen stable isotope ratio measurements of halogen- and sulfur-bearing organic compounds using elemental analyzer-chromium/high-temperature conversion isotope ratio mass spectrometry (EA-Cr/HTC-IRMS). Rapid Commun. Mass Spectrom. 31, 474–484.

Gong, B., Zheng, Y.-F., Chen, R.-X., 2007. TC/EA-MS online determination of hydrogen isotope composition and water concentration in eclogitic garnet. Phys. Chem. Miner. 34, 687–698.

Greenwood, J.P., Itoh, S., Sakamoto, N., Vicenzi, E., Yurimoto, H., 2008. Hydrogen isotope evidence for loss of water from Mars through time. Geophys. Res. Lett. 35, L05203. https://doi.org/10.1029/2007GL032721.

Greenwood, J.P., Itoh, S., Sakamoto, N., Warren, P., Taylor, L., Yurimoto, H., 2011. Hydrogen isotope ratios in lunar rocks indicate delivery of cometary water to the Moon. Nat. Geosci. 4, 79–82.

Hallis, L., et al., 2012. Magmatic water in the martian meteorite Nakhla. Earth Planet. Sci. Lett. 359-360, 84.

Higashi, Y., Itoh, S., Hashiguchi, M., Sakata, S., Hirata, T., Watanabe, K., Sakaguchi, I., 2017. Hydrogen diffusion in the apatite-water system: fluorapatite parallel to the c-axis. Geochem. J. 51, 115–122.

Jones, R.H., et al., 2014. Phosphate minerals in LL chondrites: a record of the action of fluids during metamorphism on ordinary chondrite parent bodies. Geochim. Cosmochim. Acta 132, 120–140.

Jones, R.H., et al., 2016. Phosphate minerals in the H group of ordinary chondrites, and fluid activity recorded by apatite heterogeneity in the Zag H3-6 regolith breccia. Am. Mineral. 101, 2452–2467.

Leshin, L.A., 2000. Insights into martian water reservoirs from analyses of martian meteorite QUE94201. Geophys. Res. Lett. 27, 2017–2020.

Martin, E., et al., 2017. Hydrogen isotope determination by TC/EA technique in application to volcanic glass as a window into secondary hydration. J. Volcanol. Geotherm. Res. https://doi.org/10.1016/j.jvolgeores.2017.10.013.

McCanta, M.C., et al., 2008. The LaPaz Icefield 04840 meteorite: mineralogy, metamorphism, and origin of an amphibole- and biotite-bearing R chondrite. Geochim. Cosmochim. Acta 72, 5757–5780.

McCubbin, F.M., Jones, R.H., 2015a. Extraterrestrial apatite: planetary geochemistry to astrobiology. Elements 11 (3), 183–188.

McCubbin, F.M., et al., 2010a. Nominally hydrous magmatism on the Moon. Proc. Natl. Acad. Sci. 107 (25), 11223–11228.

McCubbin, F.M., Steele, A., Nekvasil, H., Schnieders, A., Rose, T., Fries, M., Carpenter, P.K., Jolliff, B.L., 2010b. Detection of structurally bound hydroxyl in fluorapatite from Apollo Mare basalt 15058,128 using TOF-SIMS. Am. Mineral. 95, 1141–1150.

McCubbin, F.M., et al., 2012. Hydrous melting of the martian mantle produced both depleted and enriched shergottites. Geology 40, 683–688.

Nadeau, S.L., Epstein, S., Stolper, E., 1999. Hydrogen and carbon abundances and isotopic ratios in apatite from alkaline intrusive complexes, with a focus on carbonatites. Geochim. Cosmochim. Acta 63, 1837.

Nair, S., et al., 2015. Isotopic disproportionation during hydrogen isotopic analysis of nitrogen-bearing organic compounds. Rapid Commun. Mass Spectrom. 29, 878–884.

Piccoli, P.M., Candela, P.A., 2002. Apatite in igneous systems. Rev. Mineral. Geochem. 48, 255–292.

Qi, H., et al., 2010. Novel silver-tubing method for quantitative introduction of water into high-temperature conversion systems for stable hydrogen and oxygen isotopic measurements. Rapid Commun. Mass Spectrom. 24, 1821–1827.

Qi, H., et al., 2017. New biotite and muscovite isotopic reference materials, USGS57 and USGS58, for δ^2H measurements-A replacement for NBS 30. Chem. Geol. 467, 89–99.

Renpenning, J., et al., 2015. Compound-specific hydrogen isotope analysis of heteroatom-bearing compounds via gas chromatography-chromium-based high-temperature conversion (Cr/HTC)-Isotope Ratio Mass Spectrometry. Anal. Chem. 87, 9443–9450.

Robinson, K.L., Taylor, G.J., 2014. Heterogeneous distribution of water in the Moon. Nat. Geosci. 7, 401–408.

Robinson, K.L., et al., 2016. Water in evolved lunar rocks: evidence for multiple reservoirs. Geochim. Cosmochim. Acta 188, 244–260.

Sarafian, A.R., et al., 2014. Early accretion of water in the inner solar system from a carbonaceous chondrite-like source. Science 346, 623–626.

Sarafian, A.R., et al., 2016. Chlorine and hydrogen degassing in Vesta's magma ocean. Earth Planet. Sci. Lett. 459, 311–319.

Sarafian, A.R., et al., 2017. Early accretion of water and volatile elements to the inner solar system: evidence from angrites. Phil. Trans. R. Soc. A 375, 20160209. https://doi.org/10.1098/rsta.2016.0209.

Scott, J.A.J., et al., 2015. Insights into the behaviour of S, F, and Cl at Santaguito Volcano, Guantemala, from apatite and glass. Lithos 232, 375–394.

Sharp, Z.D., Atudorei, V., Durakiewicz, T., 2001. A rapid method for determination of hydrogen and oxygen isotope ratios from water and minerals. Chem. Geol. 178, 197–210.

Singer, J.A., Greenwood, J.P., Itoh, S., Sakamoto, N., Yurimoto, H., 2017. Evidence for the solar wind in lunar magmas: A study of slowly-cooled samples of the Apollo 12 olivine basalt suite. Geochem J. 51, 95–104.

Tartése, R., Anand, M., 2013. Late delivery of chondritic hydrogen into the lunar mantle: Insights from mare basalts. Earth Planet. Sci. Lett. 361, 480–486.

Tartèse, R., et al., 2013. The abundance, distribution, and isotopic composition of hydrogen in the Moon as revealed by basaltic lunar samples: Implications for the volatile inventory of the Moon. Geochim. Cosmochim. Acta 122, 58–74.

Tartèse, R., et al., 2014a. H and Cl isotope systematics of apatite in brecciated lunar meteorites Northwest Africa 4472, 773, Sayh al Uhaymir 169, and Kalahari 009. Meteorit. Planet. Sci. 1–24. https://doi.org/10.1111/maps.12398.

Tartèse, R., Anand, M., McCubbin, F.M., Elardo, S.M., Shearer, C.K., Franchi, I.A., 2014b. Apatite in lunar KREEP basalts: the missing link to understanding the H isotope systematics of the Moon. Geology 42, 363–366.

Watson, L.L., et al., 1994. Water on Mars: clues from deuterium/hydrogen and water contents of hydrous phases in SNC meteorites. Science 265, 86–90.